Head Injury Risk Assessment Considering Real Statistical Distribution Of Sheet Metal Thickness And Material Properties

Andres-Amador Garcia-Granada [1*], Horacio Rostro-Gonzalez [1]

[1]*Grup d'Enginyeria en Producte Industrial, (GEPI), Institut Químic de Sarrià, Universitat Ramon Llull, Via Augusta 390,08070 Barcelona, Spain (E-mail: andres.garcia@iqs.url.edu)*

DOI: https://doi.org/10.46720/FWC2023-SCA-012

ABSTRACT: Head injury criteria is evaluated considering different equations based on the acceleration of the impact head. The main objective it to decelerate the head from an initial impact velocity with a low deceleration. This implies the design of deformation elements in both exterior of the car for pedestrian impact and interior of the car for regulations such as ECE-R 21 or FMVSS201u. Such deformation elements should produce an optimal deceleration of the impact head. To use the minimum space for deformation, this deceleration should be as close as possible to a constant value. If we design too soft elements the injury values increase as the headform hits the stiff car structure. If we design too hard elements deceleration increases and this also means injury number increases. In real automotive parts, there is a statistical distribution of thickness and material properties that are known by quality inspection.

In this paper we present a design approach to decide the number of simulations required to be carried out to obtain an estimation of percentage of injury numbers which do not meet the requirements. Iterations in design are evaluated and discussed with particular attention to the point where engineers ask for more space for deformation. Discussion on stability of injury values is given as for example from 100 simulations only 19 injury values do not meet the requirements. This means 81% meet the requirement, but we cannot accept a 19% possibility of failure. The major discussion is to convince the engineering team of this possibility of failure when we have just a prototype test with a good injury value. This discussion is focused on the search of designs with a lower standard deviation to ensure all values meet the requirements.

Simulations of head impact are performed using Python scripts to feed the ESI Crash input deck model from real statistical values. These simulations provide as outcomes injury values with real statistical distributions which are far from normal bell shape distribution. The best design with the minimum required space to obtain a 0% failure is obtained with this approach.

KEY WORDS: HIC, risk, pedestrian, statistics, Montecarlo, FEM

1. Introduction

Designing a device involves a multitude of factors to consider, including ensuring the device's stiffness, heat resistance, and durability. In certain situations, the design must also account for impact energy absorption to reduce harm to both the object and individuals who may encounter it. To minimize this damage, specific criteria are defined, such as maximum force, torque, penetration displacement, or acceleration curve-based criteria, such as the Head Injury Criteria (HIC) or Brain Injury Criteria (BrIC), as established by Mueller et al. [1] in terms of probability. Hendre et al. [2] conducted a study on occupant injury classification, in which they utilized the Abbreviated Injury Scale (AIS) score. This score denotes the relative risk of a "threat to life" in an average person who sustains the specific coded injury as their only injury. Toganel et al. [3] compared a3ms and HIC values to determine the worst case scenario for airbag deployment. HIC is a complex equation (1) which requires to integrate acceleration using different intervals of time until we obtain a maximum value:

$$HIC = \max_{(t_1, t_2)} \left[(t_2 - t_1) \left(\frac{1}{t_2 - t_1} \int_{t_1}^{t_2} a(t)\, dt \right)^{2.5} \right] \quad (1)$$

where $a(t)$ is acceleration in g as function of time ant t_1 and t_2 are start and end time for integration in seconds. Some legislations include that this time interval should be less than 36 ms and other less than 15 ms. Units of HIC are therefore seconds.

If we hold a constant deceleration of 100g for 10 ms = 0.01 s we obtain a simple $0.01*100^{2.5}$=1000 s which is a common value adopted by many legislations. To simplify, if we assume gravity to be 9.81 m/s^2 then with 100g=981 m/s^2 in 10 ms we decelerate from 981*0.010=9.81 m/s = 35.32 kph. Once again assuming a simple constant deceleration we require to stop $0.5*981*0.010^2$=0.049 m = 49 mm.

However, it is very difficult to obtain a constant deceleration curve and therefore designers require more space to stop impact object to assure meeting legislation requirements. If we consider an elastic impact where force is a linear function of displacement the required deformation space is doubled [4].

Wei et al. [5] studied the optimization and tolerance prediction of sheet metal forming process using response surface model using hardening exponent, yield strength and friction coefficient as main noise factors. Zein et al [6] provided thickness variations due to stamping showing large scatter of thickness. Liu et al. [7] studied the effect of tolerances in sheet metal assemblies using a Montecarlo approach and Nastran simulations to evaluate the effects of deformation on component tolerances using linear mechanics. In this paper we will use a Montecarlo approach to feed ESI Pamcrash simulations to guarantee HIC values for pedestrian protection to meet regulation.

For the particular case of pedestrian protection Shojaeefard et al. [8] in 2014 compared different geometries of energy absorption systems with deterministic thickness and yield stress. Torkestani et al. [9] studied hood material type (aluminium, steel, carbon fibre epoxy CF/EP and glass fibre epoxy GF/EP composites) on the pedestrian HIC but also using a deterministic approach. Masoumi et al. [10] studied different impact locations for steel, aluminium and composite bonnet. They obtained always some points with HIC above 1000 with displacements above 50 mm. Brokman et al. [11] provided a methodology for stochastic simulation of head impacts on windshields. They studied the stochastic of glass failure and the influence on HIC. Diez et al. [12] performed simulations and tests with stochastic simulations to understand differences with nominal velocity and location. Finally, Matsumoto et al. [13] studied impacts around nominal point within 10 mm and impact velocity within ±0.7 kph. However, they found larger variation in experimental test because of variation in thickness of products, gap, test conditions and so on. In this research we want to provide an answer to the scatter shown in experimental tests.

The aim of this paper is to develop a methodology for controlling the force required to assemble parts, even when there are variations in the tolerances of deformation elements. The ability to maintain consistent force is critical in ensuring that assemblies meet the required specifications and function reliably over time. The proposed methodology considers the variations in part tolerances and deformation elements and provides a systematic approach for adjusting the force to compensate for these variations. By ensuring that the force is controlled within the desired range, the methodology enables designers and engineers to achieve high-quality assemblies that meet the required performance criteria-

1.1. Pedestrian protection: Head impact

For this research we used an old adult head of mass 4.8 kg with impact velocity of 9.72 m/s = 35 kph. Requirements specify that HIC limited to 36 ms should be less than 1000. Head impact to external car structure is very short, only a few milliseconds of contact. Then, using either 15 ms or 36ms pulse window provides the same HIC value. As the pulse itself is so short time wise, there is no risk to loose part of the pulse during calculation when applying a 15 ms interval and thus arrive to a lower calculated HIC value. This means the level of HIC 1000 can be kept and does not need to be amended to a lower value. For safety reasons all iterations are carried out considering HIC 800. In this way, values obtained over 1000 are plotted in red, values between 800 and 1000 are plotted in orange and only values below 800 are plotted in green as safe. The initial question we aim to address is the amount of space and time needed to bring a pedestrian's head to a stop, assuming a constant deceleration. This question is crucial in understanding the severity of head injuries that may occur in high-impact events involving pedestrians, such as vehicle collisions or falls from a height.

The initial step in this analysis is to determine the necessary acceleration to bring the head to a stop within 36 milliseconds of impact. For this calculation a spreadsheet is used considering g=9.81 m/s^2. We estimate that with $a=v/t$=9.72/0.036= 270m/s^2=27.54g we can stop the head using 174.96mm and obtaining a HIC value of 143.25 s. Table 1 provides a comprehensive overview of the theoretical values for acceleration, displacement, impact time, and HIC scores, ranging from the minimum acceleration required to stop the head within 36 ms to the maximum acceleration that would result in an HIC score of 1000. As shown in Table 1, an acceleration of 100g produces an HIC score of 991.33, requiring only 9.91 ms to bring the head to a stop. This result is consistent with the estimated time of 10 ms mentioned earlier.

Table 1 Constant deceleration theoretical values for 35kph

acceleration	x	t	HIC
g	mm	ms	s
27.54	174.96	36	143.25
40	120.45	24.78	250.79
60	80.30	16.52	460.73
80	60.22	12.39	709.34
86.68	55.58	11.44	800.01
100	48.18	9.91	991.33

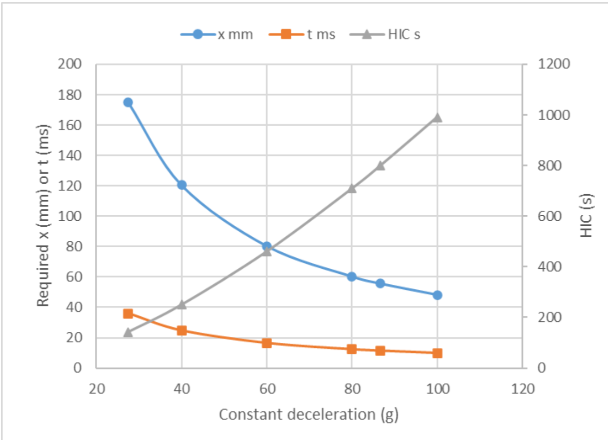

Figure 1.- Theoretical values of required space, impact time and HIC assuming constant deceleration for pedestrian impact at 35 kph

Figure 1 illustrates the impact of different constant deceleration scenarios on impact time, required space, and HIC scores. This figure provides valuable insights into the key parameters that influence the severity of head injuries sustained in high-impact events. By analyzing the relationship between deceleration, impact time, and HIC scores, we can develop more accurate finite element models and simulations that accurately represent real-world conditions. For HIC 800 we theoretically require 86.68 g, 55.58 mm and 11.48 ms.

This research paper deals with the variations in material properties of deformation elements such as thickness and yield stress. Such variations provide different deceleration values to the headform which might obtain unacceptable HIC values. To define the procedure, first the pedestrian protection impact simulation is described and then risk assessment is conducted by introducing real statistics values to deformation elements.

2. Pedestrian Protection Impact Simulation

Several finite element models were created (Figure 1) to solve head impact for different deformation space ranging from 70 to 100 mm. We used the ESI® Virtual-Performance version 2019 software on a HP Envy Laptop with a 4-core Intel® Core™ i5-10300H CPU @2.5 GHz. The software was able to generate results for node displacement, acceleration, and section forces at 5 MHz, resulting in 4,000 points for a 50 ms simulation. To capture detailed information about our models, we also recorded nodal and element data at 1 kHz, which provided us with 20 distinct time frames to analyze. The output, which included image snapshots, animated gifs, and ascii saved curves, required a storage space of 20 Mb per simulation. This streamlined process allowed us to work with different geometries in an automated fashion, following a set of numbering rules that were defined in separate include text files. Headform was provide by ESI for old legislation of mass 4.8 kg. The energy involved in all impacts is then estimated as $0.5*4.8*9.72^2= 226.8$ J.

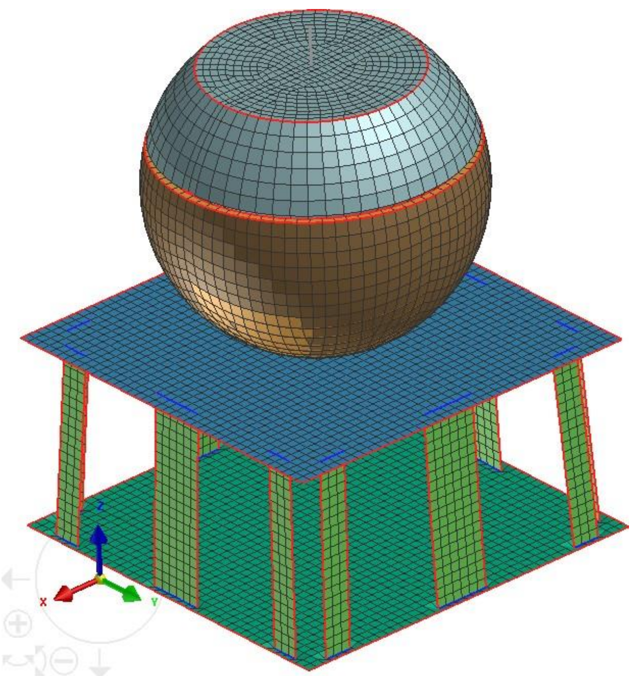

Figure 2.- Finite element model description

Deformation elements were used in the past considering PU foams of different densities. Unfortunately impacts covering different areas of the foam provided very different forces and accelerations. To avoid this, foams where covered by sheet metal parts with the mission to guarantee the area of foam to be compressed. Finally it was decided that the force could be achieved by plastic deformation of the sheet metal parts avoiding the use of the foam and reducing price an complexity of manufacturing.

Mesh element size was fixed to 5 mm which provides a stable time step of 0.9µs. Time step was dominated by headform smaller elements with a stable time step of 0.7µs. Damping which has a minor effect in stable time step was obtained according to Perez-Pena et al. [14] and fixed for all steel plates at 0.001 (0.1%). The top and lower plates shown in figure 2 measure 200 mm x 200 mm with different thickness. On each lateral side 3 connectors/columns join top and lower plate. Side legs measure 15mm in width while central leg measures 30 mm in width. All legs are slightly inclined to facilitate folding with the top joining line 5 mm inside the component at the lower part.

All plates can choose a nominal thickness of a=0.5, b=1.0, c=1.5, d=2.0 or e=2.5 mm (5 values). All plates can be designed in materials with yield stress A=0.2, B=0.4, C=0.6, D=0.8, E=1.0 or F=1.2 GP (6 values). According to these possibilities we have 30 combinations of thickness and yield stress ranging from the weakest deformation element aA for t=0.5 mm and yield 0.2 GPa to the hardest eF for t=2.5 mm and yield 1.2 GPa.

Figures 3, 4, and 5 depict different deformation elements used in our simulations. Specifically, figure 3 illustrates a weak deformation element aB with a thickness of 0.5 mm and yield strength of 0.4 GPa. In contrast, figure 4 presents an adequate deformation element bB that has a thickness of 1.0 mm and yield strength of 0.4 GPa. Lastly, figure 5 showcases a hard deformation element cB with a thickness of 1.5 mm and yield strength of 0.4 GPa. In each figure, the top left image shows the head colliding with the deformation element after 20 ms of impact. The plastic deformation in all cases ranges between 11 and 17%, which does not result in the fracture of columns. The top right image shows the energy of 226.8 J, which decreases too slowly in the case of the weak element and too quickly in the case of the hard element. The bottom left graph tracks the deceleration curve with output for HIC and a3ms. Lastly, the bottom right graph shows the force-displacement curve.

The acceleration curve depicted in figure 4 shows that it is possible to achieve a low HIC score of 336 by sustaining an acceleration of 51g. These findings align with the predictions in Table 1, assuming a constant deceleration scenario.

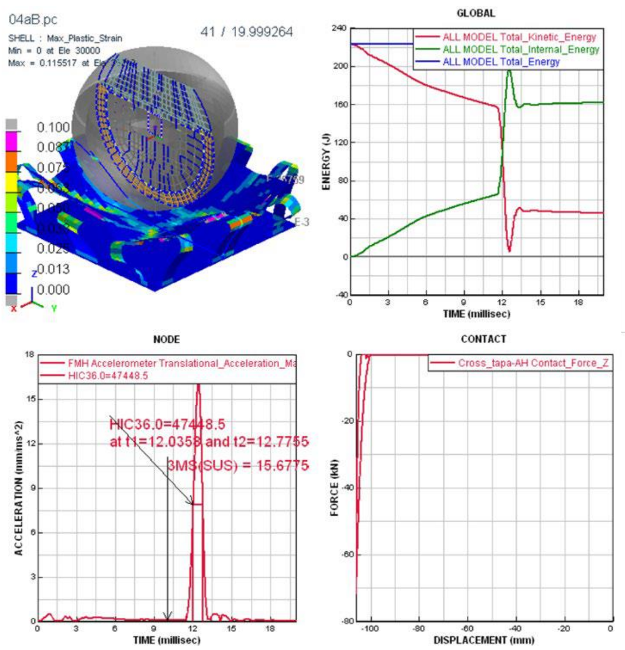

Figure 3.- Simulation for too weak case hitting the base with HIC 47448 and high force at the end using all 100mm and head rubber compression.

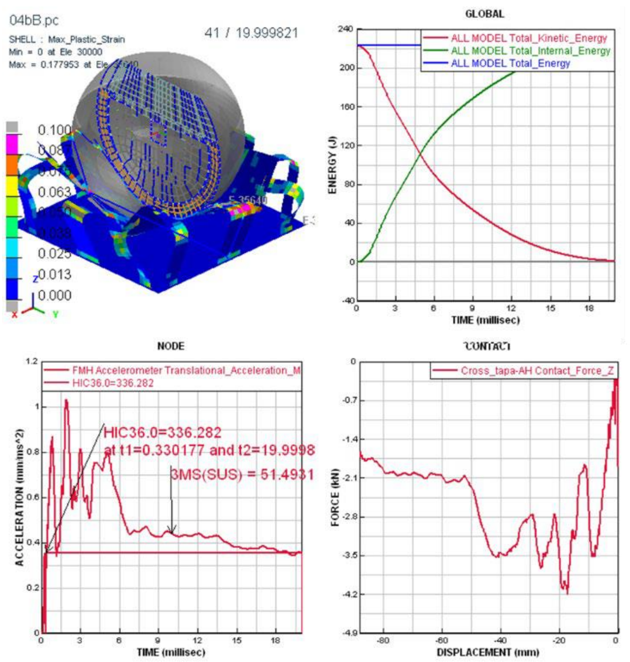

Figure 4.- Simulation for best case with HIC 336 using almost 90 mm of displacement.

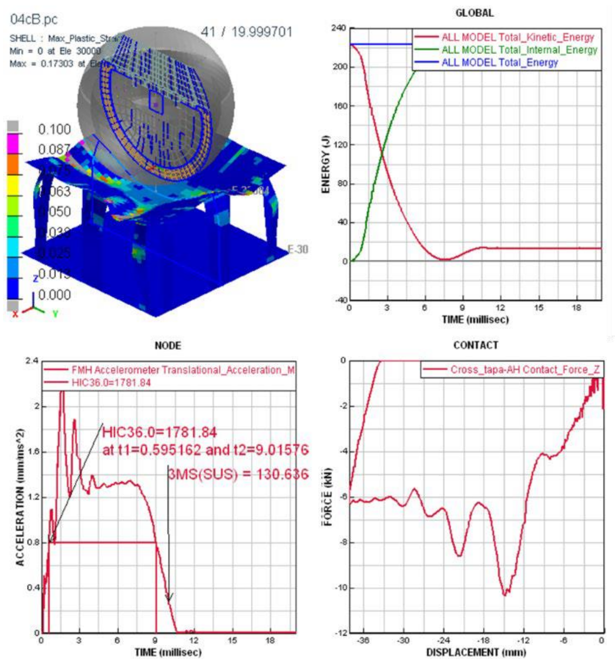

Figure 5.- Simulation for too stiff with HIC 1781 and high force at the beginning using only 38mm of displacement

After completing the simulation procedure, we proceeded to simulate 30 combinations of thickness and yield stress, along with 4 different deformation space combinations (70, 80, 90, and 100 mm).

The main objective of designers is to achieve the energy absorption with the minimum space. Figure 6 shows a3ms and HIC obtained for those 4*30=120 simulations. For 100 mm we can obtain a HIC as low as 336 for bB combination, but unfortunately this value is surrounded by red values. These means that there is a potential risk of not meeting requirements when we obtain parts with thickness and yield stress between nominal values.

100 | 80 | 79.99 | 99.99

a3ms-sust	Thickness (mm) 0.5	1	1.5	2	2.5	
Yield (GPa) 0.2	8.24512	40.1954	85.316	135.611	225.628	A
0.4	16.5002	64.2168	134.434	229.197	165.53	B
0.6	21.7353	95.29	176.907	223.168	149.236	C
0.8	26.8505	118.331	217.13	185.871	147.451	D
1	28.7057	136.963	269.553	152.569	145.86	E
1.2	33.7479	150.086	285.479	142.215	145.922	F

a3ms-sust	Thickness (mm) 0.5	1	1.5	2	2.5	
Yield (GPa) 0.2	7.55208	38.7003	83.6268	135.947	226.485	A
0.4	18.5435	64.076	132.027	229.235	164.265	B
0.6	21.6982	88.4967	165.519	230.693	155.142	C
0.8	23.9507	108.862	207.869	200.284	147.062	D
1	26.9742	130.95	235.585	174.821	145.442	E
1.2	31.9852	145.72	255.606	168.961	145.683	F

a3ms-sust	Thickness (mm) 0.5	1	1.5	2	2.5	
Yield (GPa) 0.2	7.69195	37.2212	81.1157	136.498	226.159	A
0.4	17.2586	55.3037	132.269	241.409	171.332	B
0.6	16.536	86.035	179.572	221.858	156.506	C
0.8	19.3338	106.192	213.217	185.605	149.307	D
1	22.325	121.781	252.682	154.44	148.953	E
1.2	22.7853	141.93	283.034	149.662	149.033	F

a3ms-sust	Thickness (mm) 0.5	1	1.5	2	2.5	
Yield (GPa) 0.2	7.13965	31.9823	76.3547	133.453	226.808	A
0.4	15.6775	51.4931	130.636	249.366	162.287	B
0.6	15.9049	70.5131	166.792	254.098	153.278	C
0.8	17.8998	90.0536	197.381	220.176	149.444	D
1	20.2085	113.868	223.55	198.812	148.113	E
1.2	18.4322	126.045	230.374	188.564	148.303	F
	a	b	c	d	e	

1000 | 800 | 799.9 | 999.9

HIC36	Thickness (mm) 0.5	1	1.5	2	2.5	
Yield (GPa) 0.2	66004	16010	843.142	1842.8	3769.93	A
0.4	53482.7	739.39	1873.48	4981.41	9795.8	B
0.6	44601.2	915.75	3173.45	8621.87	17042.2	C
0.8	38034.5	1400.57	4678.41	12335.9	22023.7	D
1	31200.7	1879.11	6138.17	16561.4	24546.1	E
1.2	28663.9	12335.9	7574.77	20498.4	25823.2	F

HIC36	Thickness (mm) 0.5	1	1.5	2	2.5	
Yield (GPa) 0.2	63530.9	12340.2	794.988	1835.6	3797.35	A
0.4	50460.1	493.543	1863.36	5018.45	9852.76	B
0.6	42521.5	830.456	3172.36	8542.17	17160.9	C
0.8	35266.3	1314.94	4598.63	12297.3	22290.7	D
1	28815.3	1750.41	5883.8	16572.8	24766.1	E
1.2	24418.6	12297.3	7232.45	20386.6	26041.4	F

HIC36	Thickness (mm) 0.5	1	1.5	2	2.5	
Yield (GPa) 0.2	61980.1	11057.3	765.981	1815.76	3813.3	A
0.4	48507.7	450.721	1852.48	5000.06	9846.47	B
0.6	40686.9	769.37	3151.66	8362.63	17489	C
0.8	32303.8	1166.03	4443.69	12160.7	22506.6	D
1	23919	1493.23	5725.79	16509.7	24934.8	E
1.2	20609	12160.7	6946.97	20306.8	26165.7	F

HIC36	Thickness (mm) 0.5	1	1.5	2	2.5	
Yield (GPa) 0.2	61859.6	11889.9	658.851	1805.91	3769.63	A
0.4	47448.5	336.282	1781.84	4836.25	9837.12	B
0.6	37552.9	640.271	2931.68	8164.73	17095.5	C
0.8	28016.6	958.021	4036.42	11786.4	21817.8	D
1	22983.5	1361.67	5147.51	16390.2	24220.1	E
1.2	21706.4	11786.4	6213.34	19806.8	25440.3	F
	a	b	c	d	e	

Figure 6.- Simulations for 70-, 80-, 90- and 100-mm deformation space.

3. Montecarlo Simulation

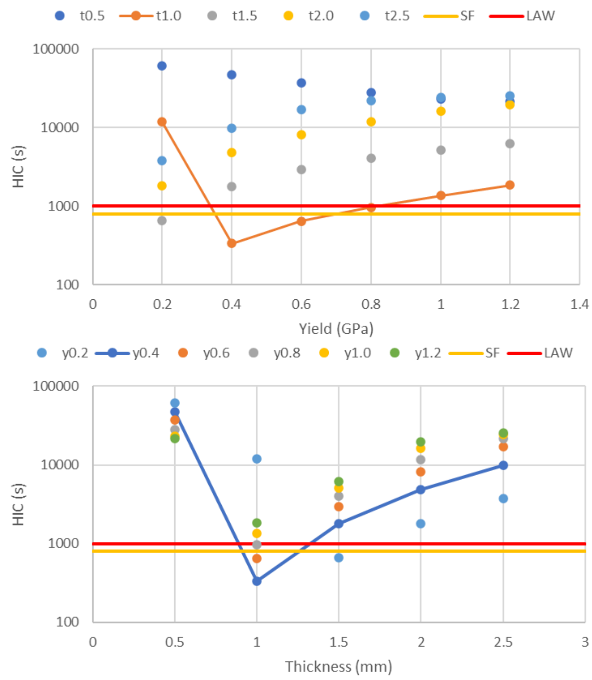

Figure 7.- Optimum design point selection for 100mm deformation space.

Figure 7 presents the same results as the bottom-right graph of Figure 6, but only for a deformation space of 100 mm and HIC. By analyzing this graph, we can observe that the bB combination (with a thickness of 1.0 mm and yield stress of 0.4 GPa) yields the optimal HIC value, which meets the legal requirements (HIC<1000) and safety criteria (HIC<800). To focus on the design points that meet these requirements, the graph is plotted using a logarithmic scale for HIC. The points to the left of the design point are considered too weak, while the points to the right are considered too hard. The solid line is drawn for the bB combination, but the exact shape of the curve is not yet fully defined to ensure that the design value is the true minimum.

Now that we have identified the bB configuration as providing acceptable values for all space configurations (as shown in Table 2), the next step is to determine the number of tests that can be conducted to meet the requirements outlined in the next section.

Table 2 HIC values for bB configuration

space	HIC
mm	s
70	739
80	494
90	451
100	336

Sheet metal parts typically come with a nominal thickness and yield stress, but these values can have some variations due to tolerances. Providers such as Arcelormittal [15] offer information on yield stress tolerances that can have an impact on the price of the material. To analyze the effect of these tolerances, we refer to Table 3, which shows the publicly available data on yield stress tolerances. By assuming the maximum value to be the average plus three times the standard deviation (σ), we can analyze the wide range of values that can be expected for the yield stress.

Table 3 Minimum, maximum and average plus standard deviation yield stress

Steel	Min yield	Max yield	Avg± σ
DX52	0.14	0.30	0.22±0.0267
DX53	0.14	0.26	0.20±0.0200
DX54	0.12	0.22	0.17±0.0167
DX56	0.12	0.18	0.15±0.0100

For this study we focus on nominal thickness *t*=1 mm with standard deviation 0.1 mm and yield 0.4 GPa with standard deviation of 0.05GPa. Using Microsoft Excel® we generate 100 thickness values for thickness and yield stress according to this normal distribution saving the number in a text file. Using a Python script 400 input deck files are generated, 100 for hic01 series using 70 mm deformation space, 100 for hic02 series with 80 mm, 100 for hic03 series with 90 mm, 100 for hic04 series with 100 mm. The main purpose is to analyse the number of values that do not meet the legal requirement depending on the available deformation space.

Figure 8 illustrates the deviation in HIC values for each series plotted as a function of yield stress and thickness. The impact of yield stress on HIC is not as pronounced as the impact of thickness. When the thickness is below 0.9 mm (-1σ), most of the data points are above the legal requirement. Moreover, there are more data points above the legal requirement for hic01 series, which only utilizes 70 mm space, compared to hic04 series where the deformation space is 100 mm.

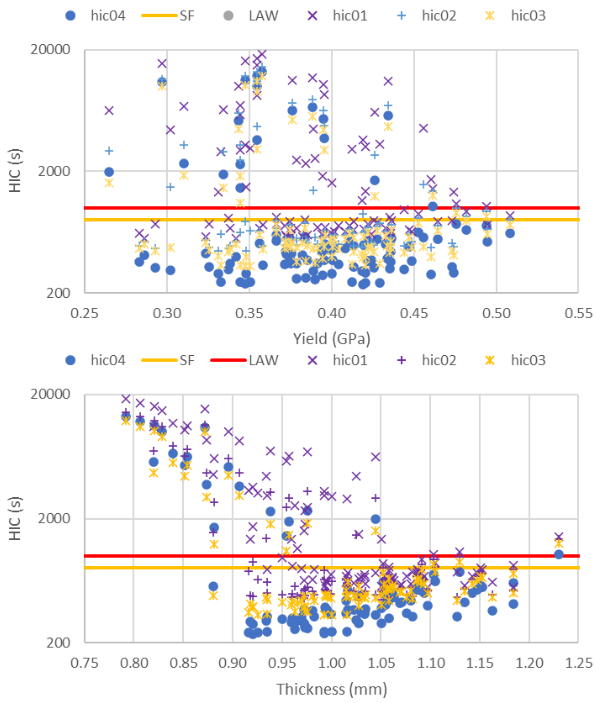

Figure 8.- HIC deviation as function of yield stress or thickness for hic01(70mm), hic02(80mm), hic03(90mm) and hic04(100mm).

Table 4 Nominal deterministic, minimum, maximum, average, standard deviation and outlaws.

Serie	Nom	Min	Max	Avg	σ*	outlaw
HIC01	739	562	18436	2932	4127	43%
HIC02	494	445	14473	1757	2928	22%
HIC03	451	335	12205	1346	2375	19%
HIC04	336	235	13220	1392	2680	19%

Table 4 shows for each series how the nominal deterministic value leads to statistical values. The average value of HIC and the percentage of points above the law is decreasing with deformation space. In this table we also plot the standard deviation calculated from each series of 100 values of HIC. It should be noted that these series do not follow a normal distribution and therefore this standard deviation value is not adequate.

Figure 9 shows the same hic values in four different plots for hic01, hic02, hic03 and hic04 series. We plot in X axis the thickness and in Y axis the yield stress. Each bubble corresponds in size to HIC value and using colour green for HIC<800, orange for 800≤HIC<1000 or red for HIC≥1000. It is possible to observe in this graph that for hic04 with 100 mm we can get all green values by designing the part with nominal thickness 1.1 mm and deviation ±0.1/3=0.033 mm and yield stress 0.425 GPa and deviation ±0.075/3=0.025 GPa. This corresponds to the square area plotted with dash lines for ±3σ. Solid square line is the original ±2σ for thickness ±2*0.1=±0.2 mm and for yield ±2*0.05=±0.1 GPa.

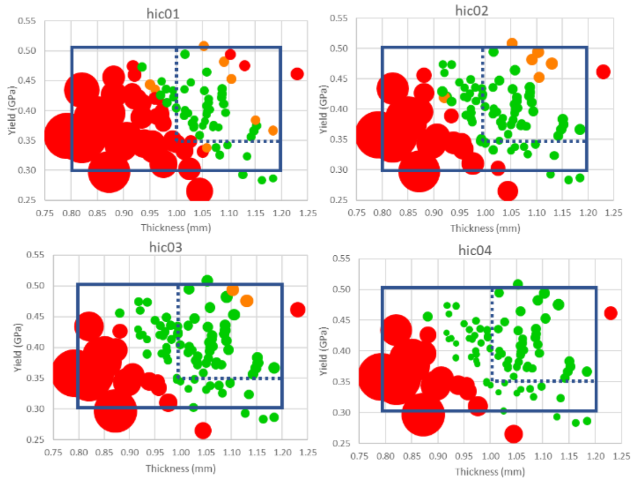

Figure 9.- HIC deviations for hic01(70mm), hic02(80mm), hic03(90mm) and hic04(100mm) colour for safety and legal requirements.

Finally, figure 10 shows the histogram distribution of HIC with interval of HIC 200s showing that this is far from normal distribution. Solid lines show accumulated values of HIC with 57 out of 100 values for hic01 below 1000 (43% failure in table 4), 78 for hic02 (22% failure) and 81 for hic03 and hic04 (19% failure).

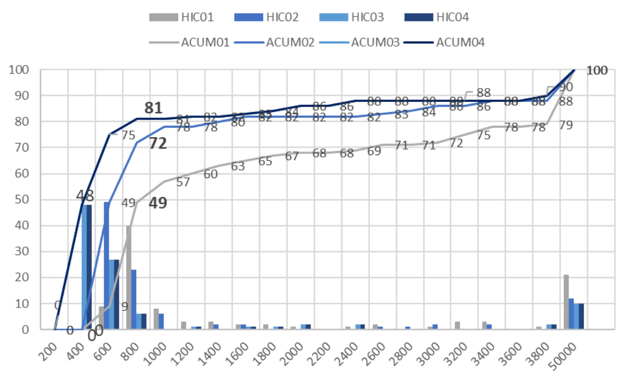

Figure 10.- Statistical HIC distributions for hic01(70mm), hic02(80mm), hic03(90mm) and hic04(100mm).

4. Conclusion

In conclusion, we have demonstrated the possibility of designing a deformation element that can decelerate an adult head with a mass of 4.8 kg traveling at 35 kph to obtain HIC values below 1000. The deformation element made of steel plates can convert kinetic energy into plastic deformation energy, and theoretical values of constant deceleration show that deformation space larger than 50 mm is required for this purpose.

Deterministic simulations were performed for a range of nominal thicknesses and yield stresses, which showed that the minimum HIC value is obtained for a thickness of 1 mm and a yield stress of 0.4 GPa. These simulations resulted in acceptable HIC values for hic01-70mm 739, decreasing to hic02-80mm 493, hic03-90mm 451 and hic04-100mm 336.

Computing 100 simulations for each series introducing a standard deviation in thickness of ±0.1mm and in yield of ±0.05 GPa lead to hic values which do not meet legal requirements. The number of possible tests which do not meet the requirements is reduced from 43% for 70 mm to 19% for 90 and 100 mm. Reducing the tolerances in thickness from ±0.1mm to ±0.033mm and in yield from ±0.05 GPa to ±0.025 GPa would achieve all points in green (HIC<800) for 100 mm space deformation and in green+orange (HIC<1000) for 80 and 90 mm. This study is not safe for 70 mm deformation space as we find red points within tolerances.

This study emphasizes the importance of risk analysis in determining the appropriate tolerances for deformation elements, which have a significant impact on price and negotiation for required deformation space. Performing just on experiment that provides an acceptable value of HIC is not a guarantee that we meet the requirement for each possible combination of thickness and yield stress. Overall, this methodology provides valuable insight into the design of deformation elements for mitigating head injuries in vehicular accidents.

References

[1] B. Mueller, A. MacAlister, J. Nolan, and D. Zuby, "Comparison of HIC and BrIC head injury risk in IIHS frontal crash tests to real-world head injuries," in *Proceedings of the 24th International Technical Conference on the Enhanced Safety of Vehicles*, 2015, pp. 1–18.

[2] K. M. Hendre, K. D. Mali, and D. M. Kulkarni, "A Study of Occupant Injuries Classification in Automobile Accidents in Relation to Upper Extremities Bones," in *Recent Advances in Mechanical Infrastructure: Proceedings of ICRAM 2019*, 2020, pp. 273–285.

[3] G.-R. Toganel and A. O. Soica, "A late and failure of airbag deployment case study for drivers of passenger cars in rear-end collisions," in *IOP Conference Series: Materials Science and Engineering*, 2017, vol. 252, no. 1, p. 12020.

[4] C. Pinecki and R. Zeitouni, "Technical solutions for enhancing the pedestrian protection," *Knee*, vol. 200, p. 150, 2007.

[5] D. Wei, Z. Cui, and J. Chen, "Optimization and tolerance prediction of sheet metal forming process using response surface model," *Comput. Mater. Sci.*, vol. 42, no. 2, pp. 228–233, 2008.

[6] H. Zein, M. El Sherbiny, M. Abd-Rabou, and others, "Thinning and spring back prediction of sheet metal in the deep drawing process," *Mater. \& Des.*, vol. 53, pp. 797–808, 2014.

[7] S. C. Liu, S. J. Hu, and T. C. Woo, "Tolerance analysis for sheet metal assemblies," 1996.

[8] M. H. Shojaeefard, A. Najibi, and M. R. Ahmadabadi, "Pedestrian safety investigation of the new inner structure of the hood to mitigate the impact injury of the head," *Thin-walled Struct.*, vol. 77, pp. 77–85, 2014.

[9] A. Torkestani, M. Sadighi, and R. Hedayati, "Effect of material type, stacking sequence and impact location on the pedestrian head injury in collisions," *Thin-Walled Struct.*, vol. 97, pp. 130–139, 2015.

[10] A. Masoumi, M. H. Shojaeefard, and A. Najibi, "Comparison of steel, aluminum and composite bonnet in terms of pedestrian head impact," *Saf. Sci.*, vol. 49, no. 10, pp. 1371–1380, 2011.

[11] C. Brokmann, C. Alter, and S. Kolling, "A Methodology for Stochastic Simulation of Head Impact on Windshields," *Appl. Mech.*, vol. 4, no. 1, pp. 179–190, 2023, doi: 10.3390/applmech4010010.

[12] M. Diez, J. J. Ferrer, J. Garc\'\ia, R. Mart\'\in, A. Negro, and F. CIDAUT, "Demonstrator for Virtual Testing Procedure. Application to Pedestrian Adult Head Impacts," 2009.

[13] T. Matsumoto, K. Kumagai, and H. Arimoto, "Development of robust Design Method in Pedestrian impact test," 2007.

[14] a. Perez-Pena, a. a. Garcia-Granada, J. Menacho, J. J. Molins, and G. Reyes, "A methodology for damping measurement of engineering materials: application to a structure under bending and torsion loading," *J. Vib. Control*, Sep. 2014, doi: 10.1177/1077546314547728.

[15] "Arcelormittal." https://industry.arcelormittal.com/catalogue/E20/EN (accessed May 02, 2023).

Acknowledgement

This work has been performed with the support of research group GEPI which stands for Industrial Product Engineering Group (Grup Enginyeria Producte Industrial) and the collaboration with ESI who provided pedestrian headform and software for simulations.